

Supplementary Materials:

# Making Landsat Time Series Consistent: Evaluating and Improving Landsat Analysis Ready Data

Shi Qiu <sup>1,2,†</sup>, Yukun Lin <sup>1,3,4,†</sup>, Rong Shang <sup>1,\*</sup>, Junxue Zhang <sup>1</sup>, Lei Ma <sup>1</sup>, and Zhe Zhu <sup>1,\*</sup>

<sup>1</sup> Department of Geosciences, Texas Tech University, Lubbock, TX 79409, United States; qsly09@hotmail.com (S.Q.); yukunlin91@gmail.com (Y.L.); kasimjxzhong@gmail.com (J.Z.); maleinju@gmail.com (L.M.);

<sup>2</sup> School of Resources and Environment, University of Electronic Science and Technology of China, Chengdu, Sichuan 611731, China;

<sup>3</sup> Institute of Remote Sensing and Digital Earth, Chinese Academy of Sciences, Beijing 100101, China;

<sup>4</sup> University of Chinese Academy of Sciences, Beijing 100049, China;

\* Correspondence: rongshang90@gmail.com (R.S.); Tel.: +1 (571) 508 9541; zhe@uconn.edu (Z.Z.); Tel.: +1 (617) 233 6031;

† Contributed equally to the work.

**This file includes:**

Table S1 and Figure S1 to S16

**Table 1.** Acronyms for supplementary materials.

Acronym	Full Spelling or Explaining
ARD	Analysis Ready Data
BRDF	Bidirectional Reflectance Distribution Function
CA	Coastal Central California (test site)
FL	Eastern Florida Coast (test site)
Fmask	Function of mask
IC	Illumination Correction
NCO	North Colorado Rockies (test site)
NH	Vermont, New Hampshire (test site)
SCS	Sun-Canopy-Sensor
SCS+C	a semiempirical SCS
SD	Standard Deviation
SR	Surface Reflectance
WA	Puget Lowlands, Washington (test site)

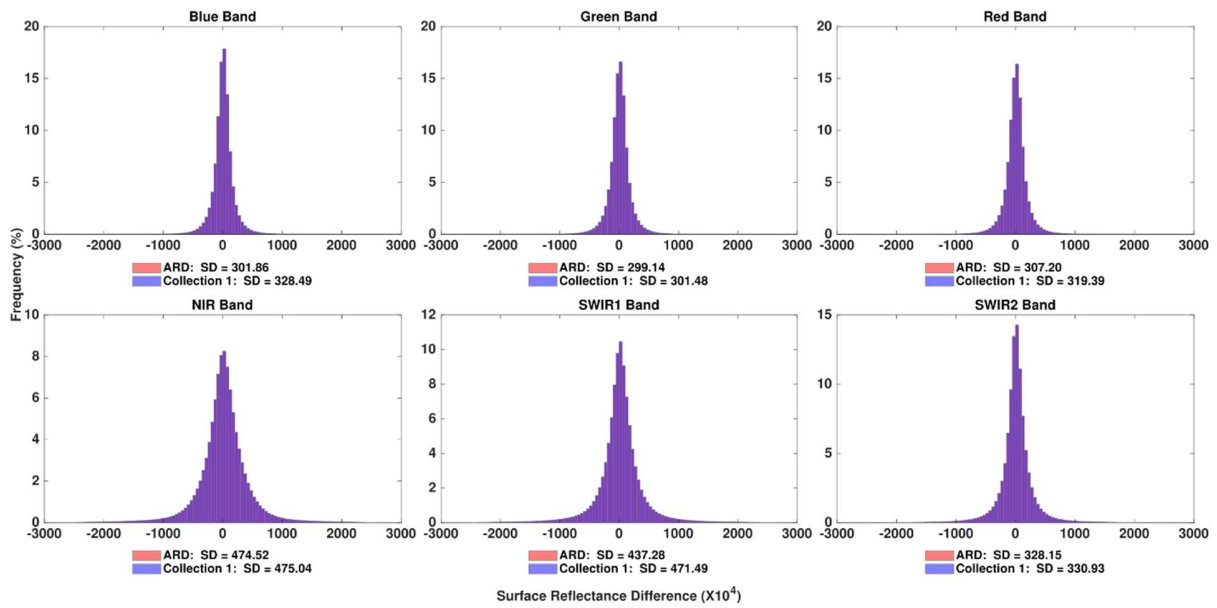


**Figure S1.** The histograms of SR difference between ARD and Collection 1 data for six Landsat spectral bands based on a total of 3.72 billion SR difference values at the FL site.

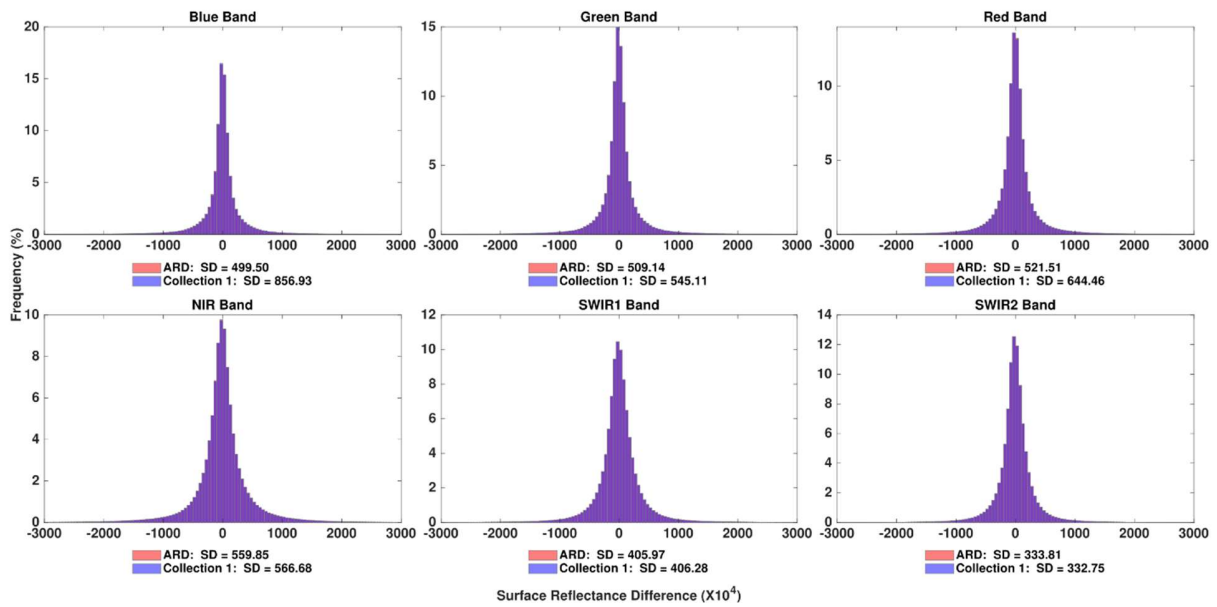


**Figure S2.** The histograms of SR difference between ARD and Collection 1 data for six Landsat spectral bands based on a total of 2.87 billion SR difference values at the NCO site.

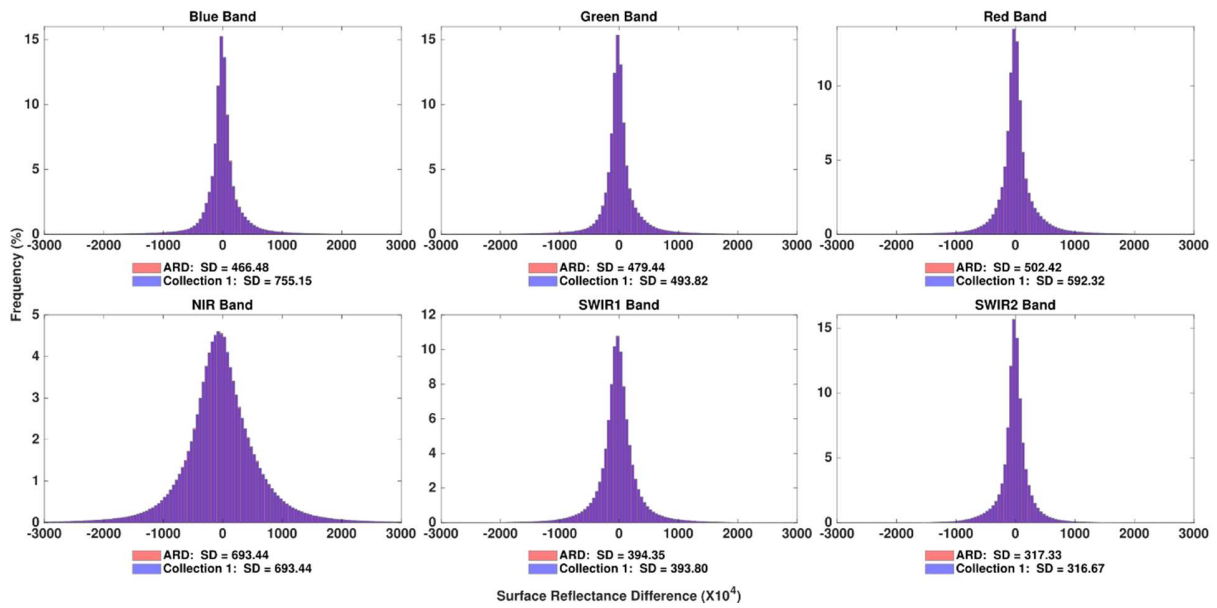


**Figure S3.** The histograms of SR difference between ARD and Collection 1 data for six Landsat spectral bands based on a total of 2.38 billion SR difference values at the NH site.

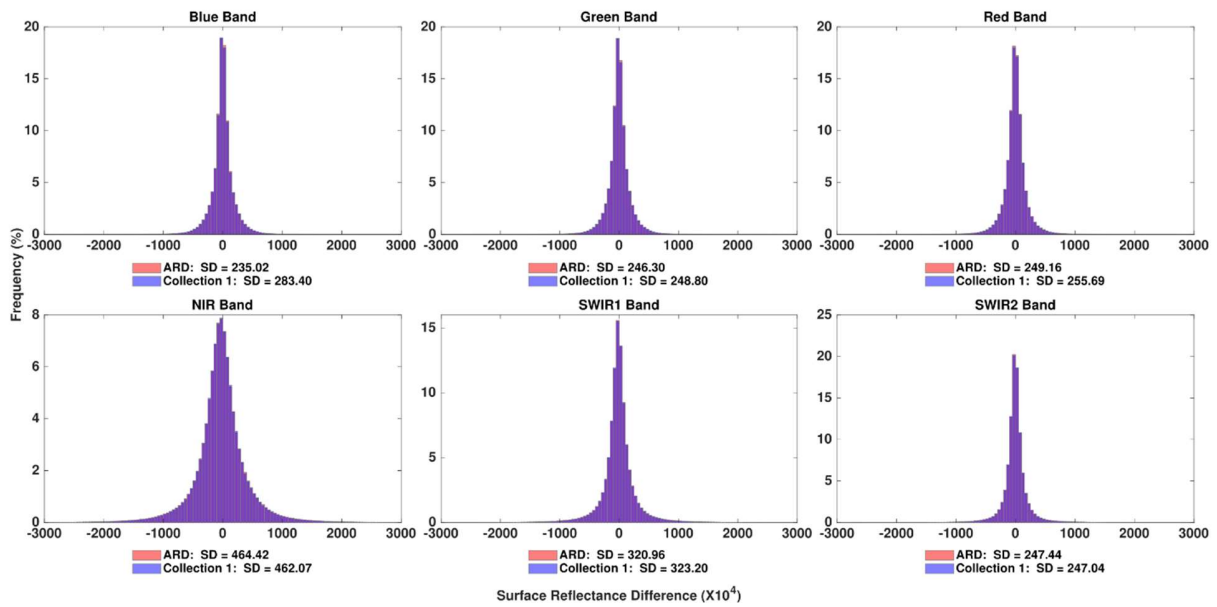


**Figure S4.** The histograms of SR difference between ARD and Collection 1 data for six Landsat spectral bands based on a total of 1.23 billion SR difference values at the WA site.

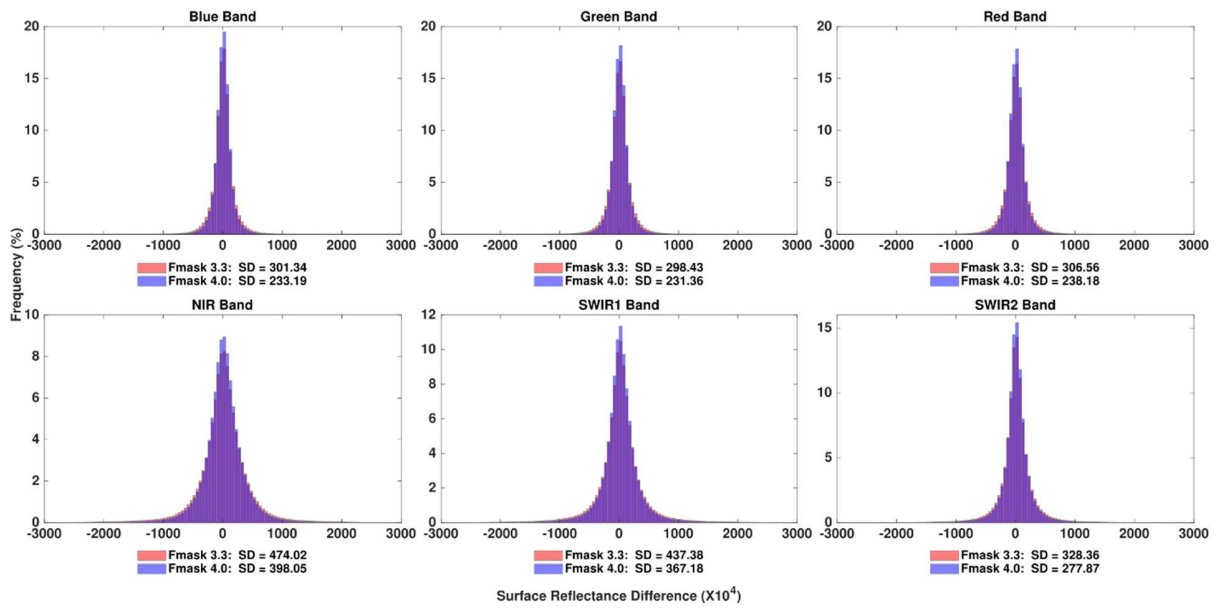


**Figure S5.** The histograms of SR difference between ARD with Fmask 3.3 (derived from 3.72 billion SR difference values) and that with Fmask 4.0 (derived from 3.16 billion SR difference values) for six Landsat spectral bands at the FL site.

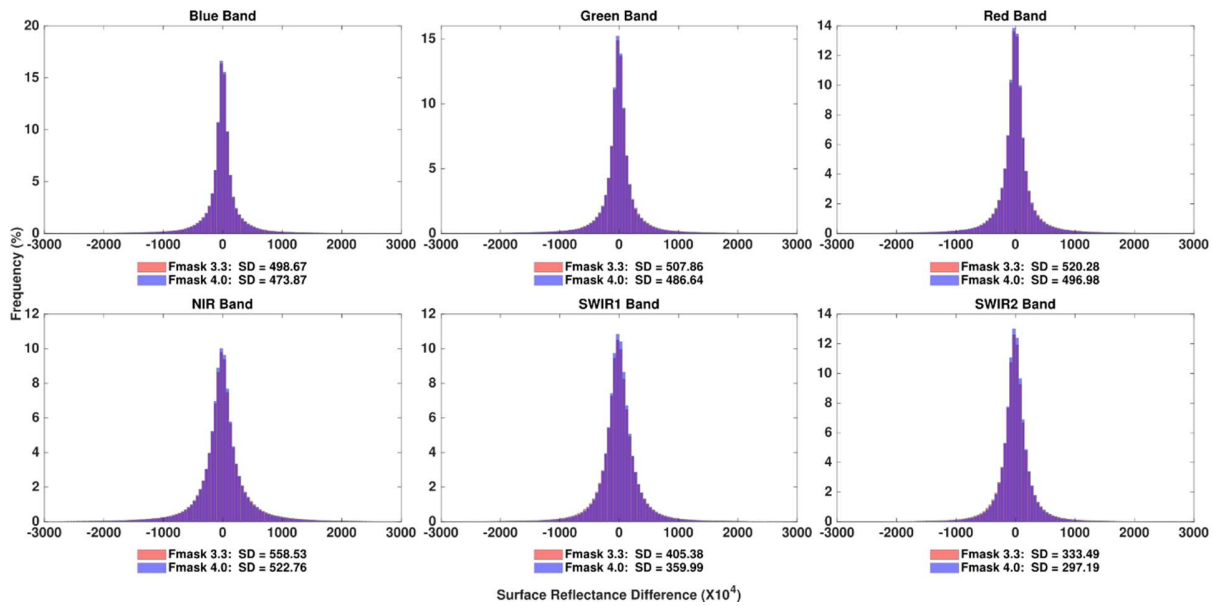


**Figure S6.** The histograms of SR difference between ARD with Fmask 3.3 (derived from 2.87 billion SR difference values) and that with Fmask 4.0 (derived from 2.75 billion SR difference values) for six Landsat spectral bands at the NCO site.

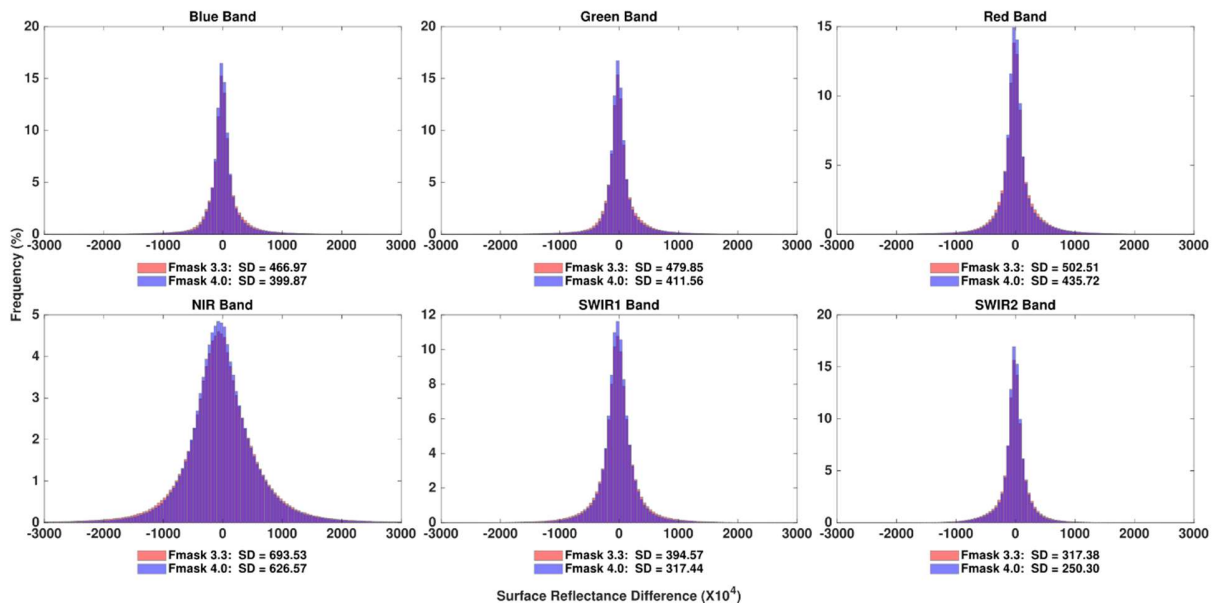


**Figure S7.** The histograms of SR difference between ARD with Fmask 3.3 (derived from 2.38 billion SR difference values) and that with Fmask 4.0 (derived from 2.06 billion SR difference values) for six Landsat spectral bands at the NH site.

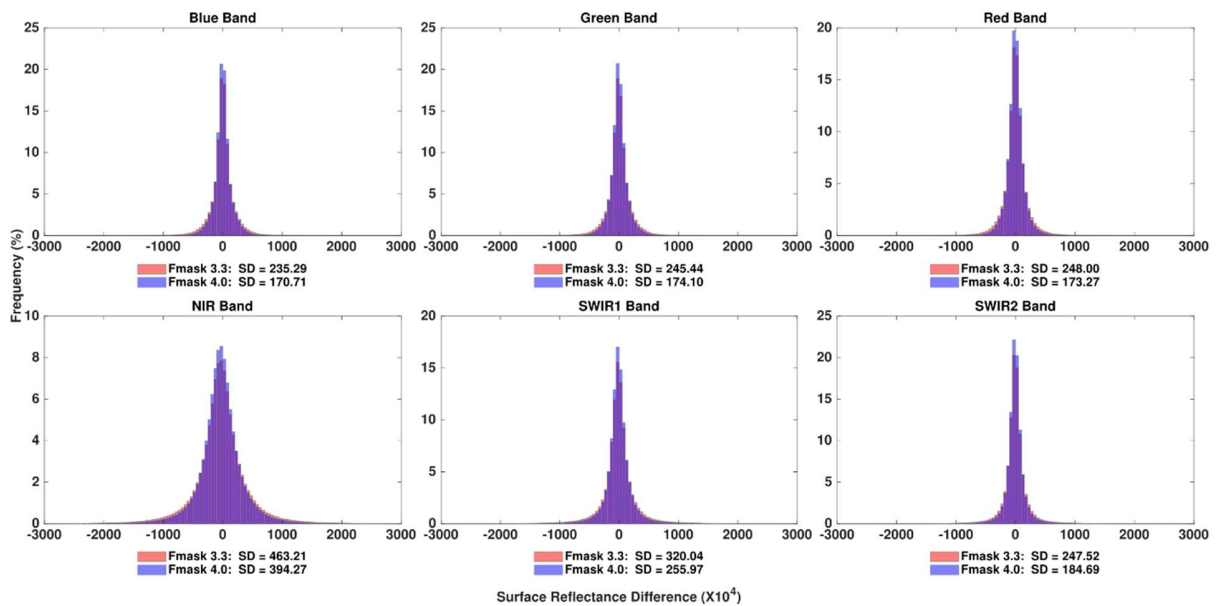


**Figure S8.** The histograms of SR difference between ARD with Fmask 3.3 (derived from 1.23 billion SR difference values) and that with Fmask 4.0 (derived from 1.07 billion SR difference values) for six Landsat spectral bands at the WA site.

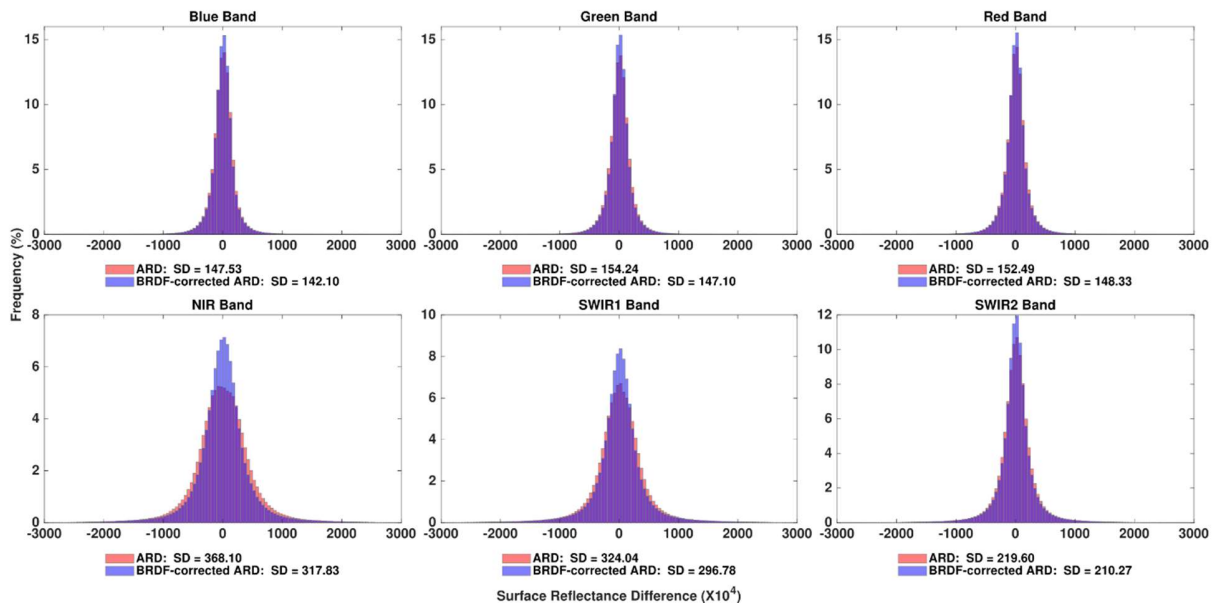


**Figure S9.** The histograms of SR difference between original ARD and BRDF-corrected ARD for six Landsat spectral bands based on a total of 2.18 billion SR difference values at the FL site.

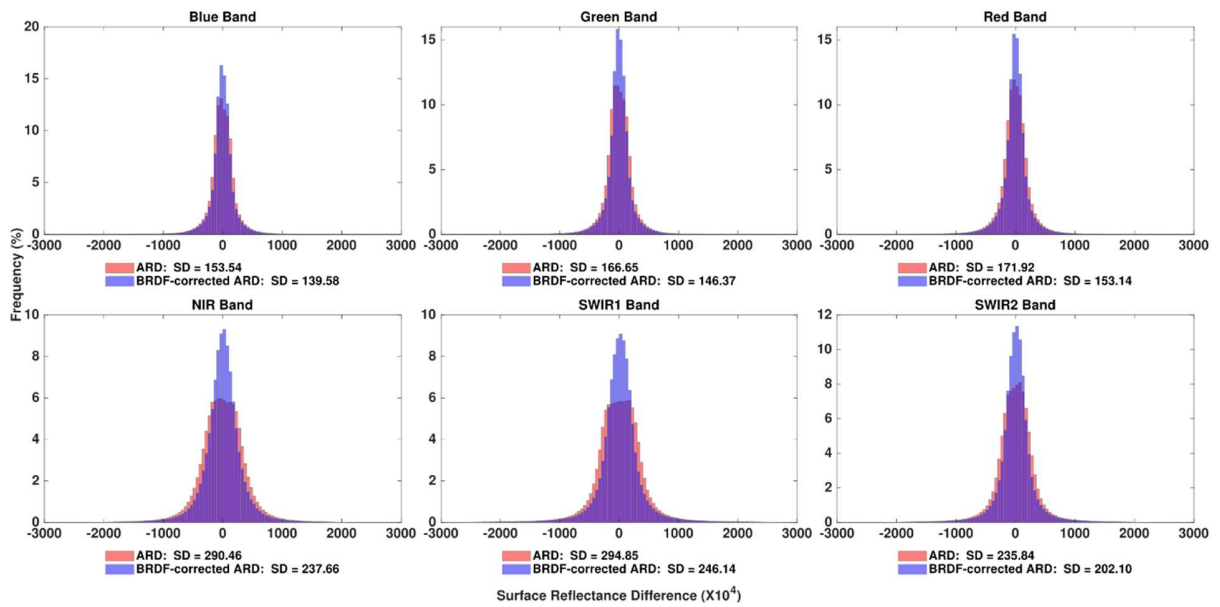


**Figure S10.** The histograms of SR difference between original ARD and BRDF-corrected ARD for six Landsat spectral bands based on a total of 2.16 billion SR difference values at the NCO site.

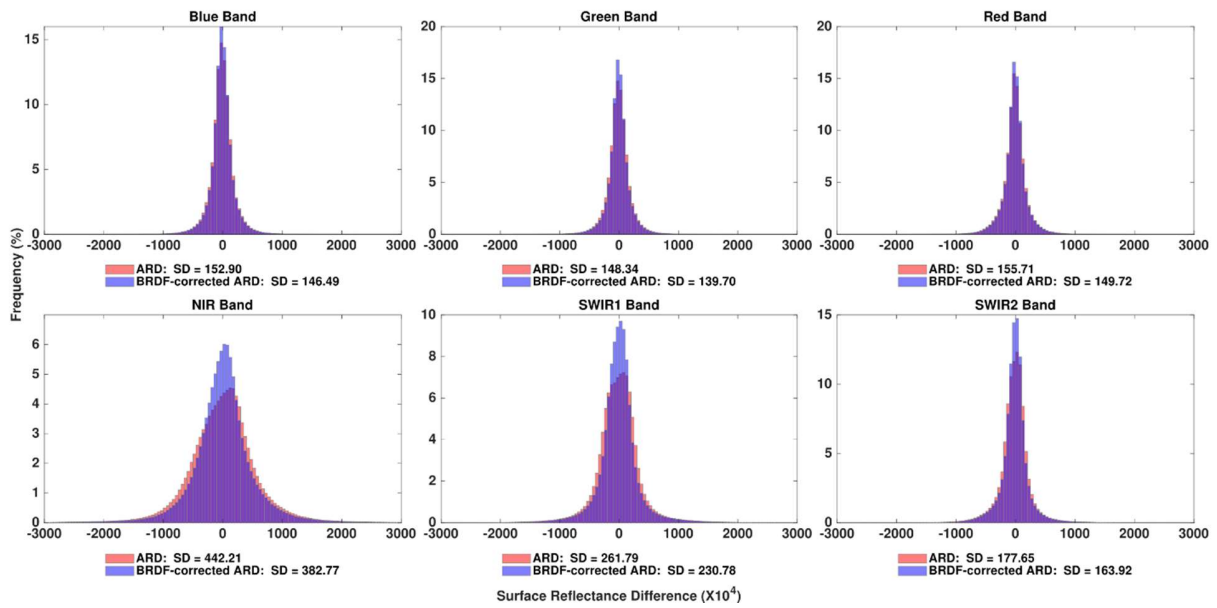


**Figure S11.** The histograms of SR difference between original ARD and BRDF-corrected ARD for six Landsat spectral bands based on a total of 1.87 billion SR difference values at the NH site.

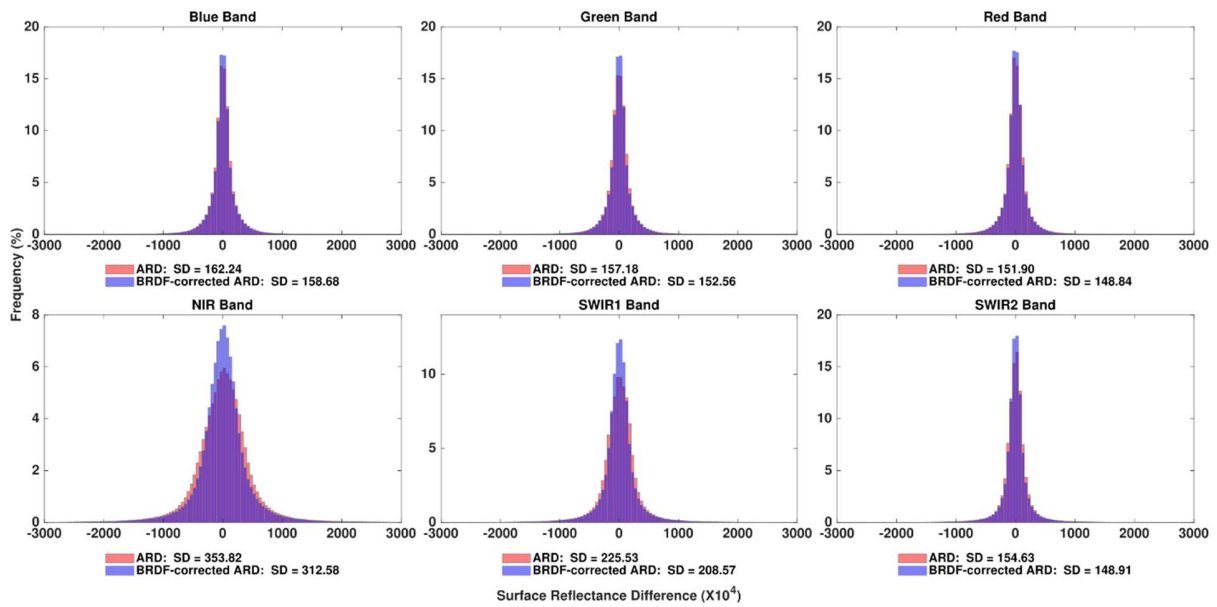


**Figure S12.** The histograms of SR difference between original ARD and BRDF-corrected ARD for six Landsat spectral bands based on a total of 1.70 billion SR difference values at the WA site.

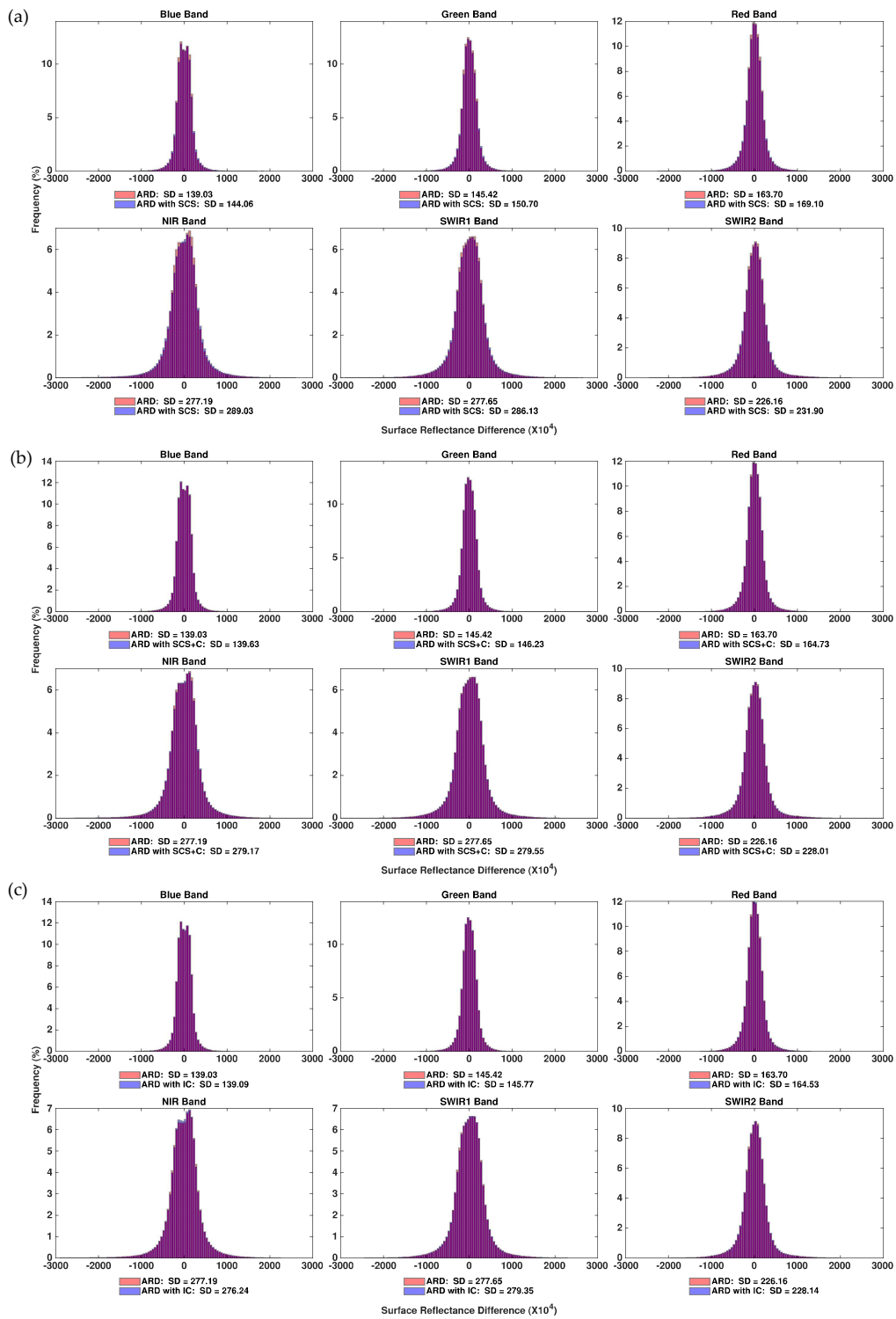


**Figure S13.** The histograms of SR difference between the topographically corrected ARD surface reflectance and original ARD surface reflectance of six Landsat spectral bands for three different methods based on a total of 4.21 billion SR difference values at the CA site. From the top to bottom are the SCS, SCS+C, IC topographic correction method.



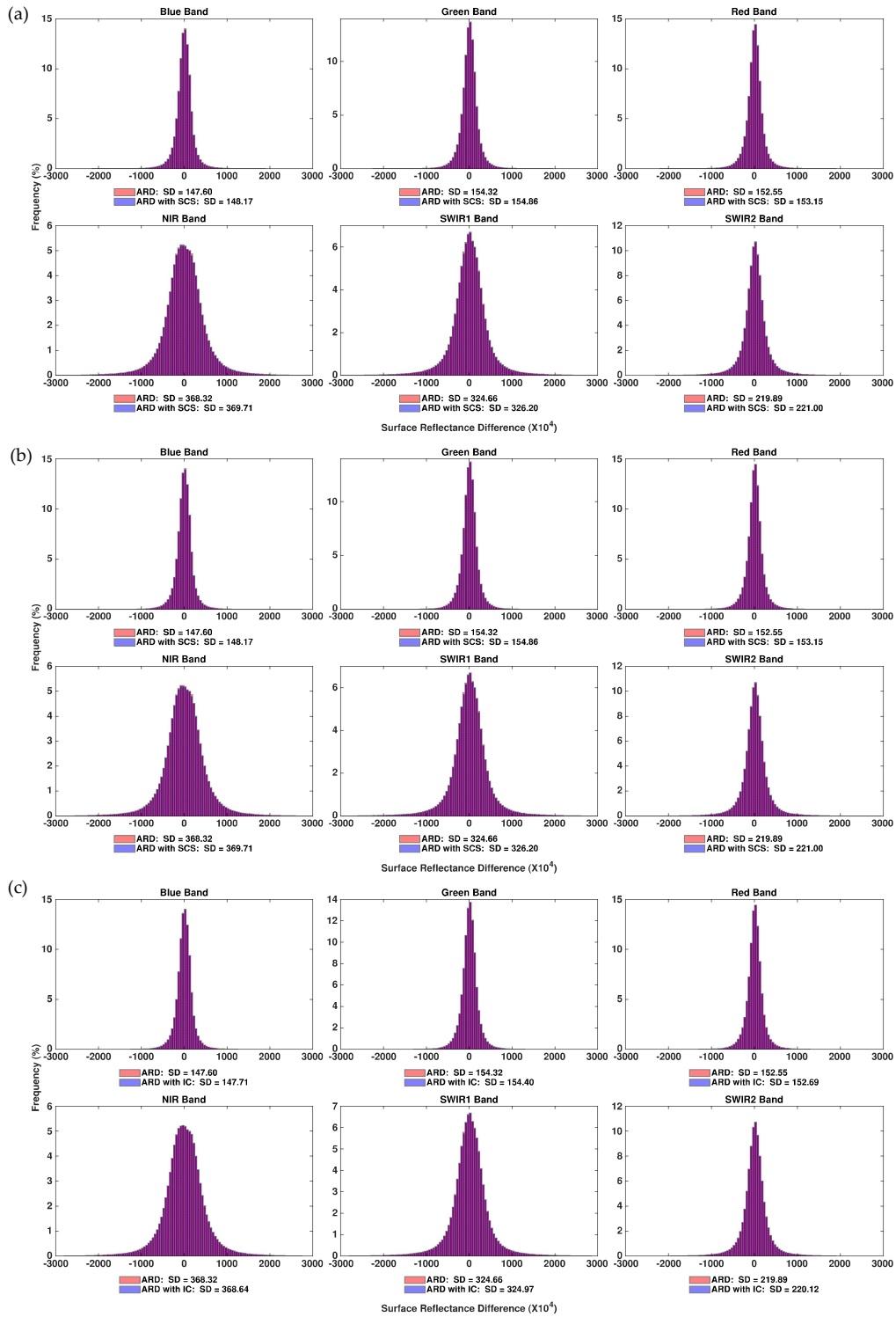


**Figure S14.** The histograms of SR difference between the topographically corrected ARD surface reflectance and original ARD surface reflectance of six Landsat spectral bands for three different methods based on a total of 2.18 billion SR differences at the FL site. From the top to bottom are the SCS, SCS+C, IC topographic correction method.

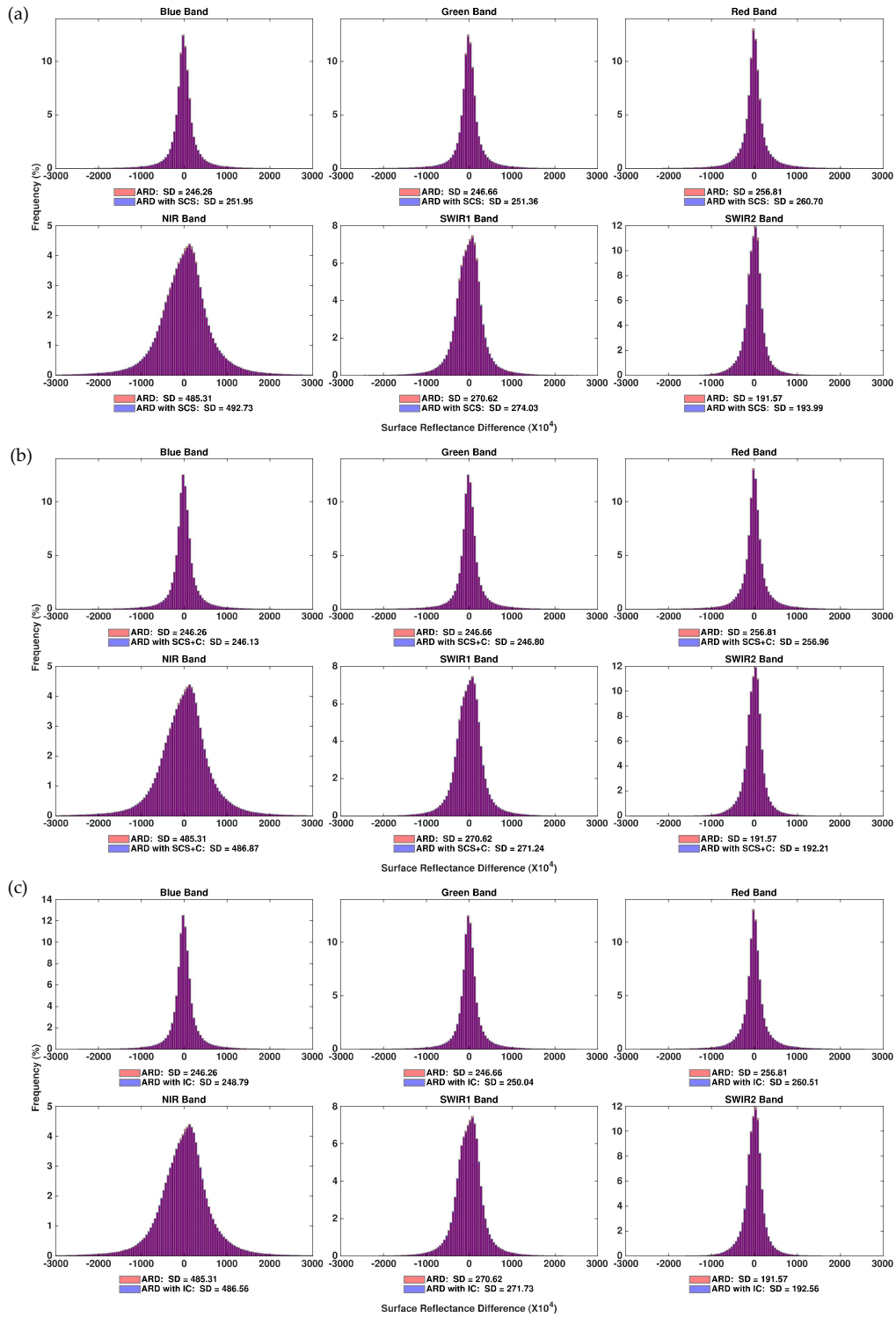


**Figure S15.** The histograms of SR difference between the topographically corrected ARD surface reflectance and original ARD surface reflectance of six Landsat spectral bands for three different methods based on a total of 2.33 billion SR differences at the NH site. From the top to bottom are the SCS, SCS+C, IC topographic correction method.

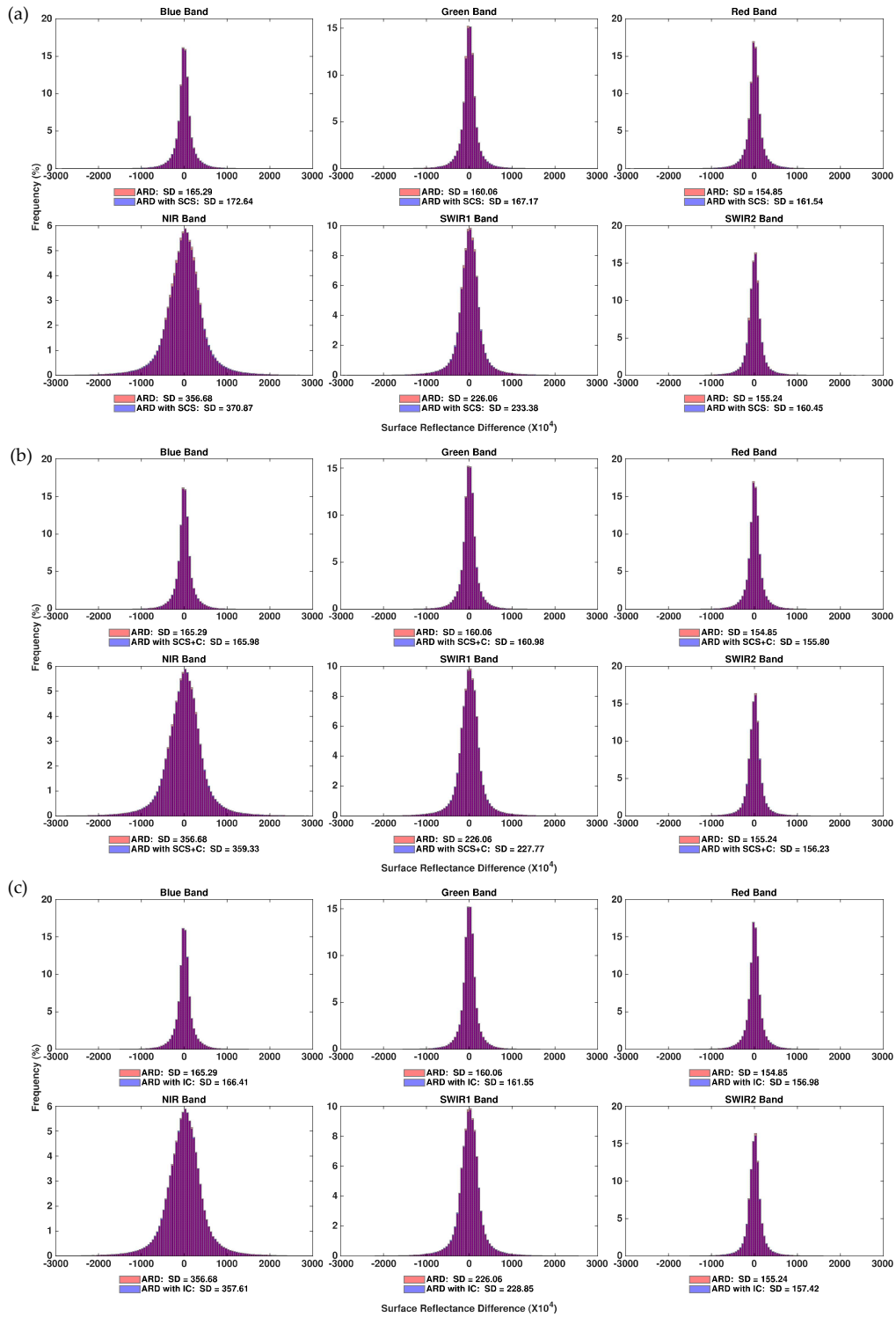


**Figure S16.** The histograms of SR difference between the topographically corrected ARD surface reflectance and original ARD surface reflectance of six Landsat spectral bands for three different methods based on a total of 1.71 billion SR differences at the WA site. From the top to bottom are the SCS, SCS+C, IC topographic correction method.